ERDC/GSL SR-17-4 rev.

Geotechnical and Structures Laboratory

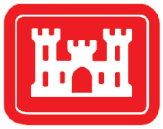

US Army Corps
of Engineers®
Engineer Research and
Development Center

ERDC
INNOVATIVE SOLUTIONS
for a safer, better world

Flood and Coastal Storm Damage Reduction Program

SWCC Prediction: Seep/W Add-In Functions

Lucas Walshire and Bryant Robbins

June 2017
(Revised November 2017)

The U.S. Army Engineer Research and Development Center (ERDC) solves the nation's toughest engineering and environmental challenges. ERDC develops innovative solutions in civil and military engineering, geospatial sciences, water resources, and environmental sciences for the Army, the Department of Defense, civilian agencies, and our nation's public good. Find out more at www.erdc.usace.army.mil.

To search for other technical reports published by ERDC, visit the ERDC online library at http://acwc.sdp.sirsi.net/client/default.

Flood and Coastal Storm Damage
Reduction Program

ERDC/GSL SR-17-4 rev.
June 2017
(Revised November 2017)

SWCC Prediction: Seep/W Add-In Functions

Lucas Walshire and Bryant Robbins

Geotechnical and Structures Laboratory
U.S. Army Engineer Research and Development Center
3909 Halls Ferry Road
Vicksburg, MS 39180-6199

Final report

Prepared for U.S. Army Corps of Engineers
Washington, DC 20314-1000

Under Project Number HFK2F2 “Development of best practices for use of transient seepage analysis in geotechnical engineering practice”

Abstract

The soil water characteristic curve (SWCC) defines a constitutive relationship between the negative pressure that develops when a soils saturation level is less than fully saturated, and the corresponding volume of water held in the pore space of the soil matrix. As this relationship is not commonly measured in geotechnical laboratories, practitioners often attempt to predict this relationship based on other commonly measured material properties using empirical prediction methods. The performance of five SWCC empirical predictors was evaluated through comparisons to independently measured SWCC data for four soils. SWCC prediction methods were selected for this investigation if they incorporated commonly measured soil properties to predict the SWCC. The error in the SWCC prediction was assessed in terms of both the mean squared error on the SWCC prediction and the impact of the error on a numerical analysis of the Green and Ampt infiltration problem. The results of the numerical analysis were assessed in terms of a normalized saturation coefficient. The normalized saturation coefficient provided a clear means of monitoring a transient seepage analysis through a single measure. Results indicate that the SWCC prediction methods yielding the lowest mean squared error did not necessarily yield the smallest error in the transient seepage analysis. Further, only the Perrera et al. method consistently yielded conservative analysis results for all soil types investigated.

Contents

Figures and Tables

Figures

Tables

Preface

This study was conducted under the Flood and Coastal Storm Damage Reduction Program. The technical monitor was Dr. Cary Talbot, Associate Technical Director, Coastal and Hydraulics Laboratory.

The work was performed by the Geotechnical and Structures Laboratory under the supervision of the Technical Directors Office (GV-T), U.S. Army Engineer Research and Development Center, Geotechnical and Structures Laboratory (ERDC-GSL). At the time of publication, Dr. Maureen K. Corcoran, CEERD-GV-T was the acting Technical Director for Water Resources Infrastructure. The Deputy Director of ERDC-GSL was Dr. William P. Grogan, and the Director was Mr. Bartley P. Durst. At the time of revision, the Acting Deputy Director of ERDC-GSL was Mr. Charles W. Ertle, and the Director was Mr. Bartley P. Durst.

COL Bryan S. Green was the Commander of ERDC, and Dr. David W. Pittman was the Director.

1 Introduction

The soil water characteristic curve (SWCC) is the relationship between the soil-water suction and the water content of the soil. This relationship helps define the magnitude of matric suction that occurs in a soil deposit when the water content is less than saturated. The quantity of water retained in a soil at a certain magnitude of suction depends on many factors: particle shape, particle size, distribution of pore spaces, mineralogy, surface activity of solid grain particles, and chemical composition of interstitial water (Aubertin et al. 2003). The SWCC is important in geotechnical engineering, as the degree of saturation and corresponding matric suction greatly influences the shear strength and hydraulic conductivity of soils. A partially saturated soil will have a decreased hydraulic conductivity and increased shear strength as compared to a saturated soil.

A series of SWCC prediction methods was investigated to ascertain which would be appropriate for use on preliminary analyses of U.S. Army Corps of Engineers (USACE) projects, such as dams and levees. SWCC prediction methods were selected for this investigation if they incorporated commonly measured soil properties to predict the SWCC. It is more desirable to directly measure the SWCC in the laboratory, but this type of testing is not commonplace in practice.

In the literature, five SWCC prediction methods that use common soil properties for curve estimation were found. The soil properties used by the selected prediction methods were saturated hydraulic conductivity, grain size, plasticity index, and porosity. The finite element seepage program Seep/W©, distributed by GeoStudio, was used as the platform for the developed Add-In functions. Each prediction method was programmed as a function and compiled as a digital library (*.dll). The performances of the five SWCC prediction methods were evaluated by comparing the predicted curves to independent laboratory measurements. Finally, the significance of the errors associated with the SWCC predictions was assessed through a numerical transient seepage analysis.

2 General Characteristics of the SWCC

The difference between steady state and transient seepage analysis is that no parameters vary with time during a steady state analysis. In a transient seepage analysis, the hydraulic boundary conditions, volumetric water content, and hydraulic conductivity all vary temporally. Hydraulic conductivity is related to the volumetric water content (and corresponding matric suction) through the hydraulic conductivity function, which is typically predicted from the SWCC. Increasing suction (decreasing saturation) decreases soil permeability. Therefore, it is important to understand how to accurately estimate the SWCC for a transient seepage analysis. The following sections will focus solely on the influence of SWCC in the context of transient seepage analysis.

The governing differential equation for three-dimensional seepage is shown in Equation 1:

$$\frac{\partial}{\partial x}\left[k_x(\theta)\frac{\partial H}{\partial x}\right]+\frac{\partial}{\partial y}\left[k_y(\theta)\frac{\partial H}{\partial y}\right]+\frac{\partial}{\partial z}\left[k_z(\theta)\frac{\partial H}{\partial z}\right]+Q=\frac{\partial \theta}{\partial t} \quad (1)$$

where Q is a boundary flux, H is total head, k_n is hydraulic conductivity in the n direction (n is either x, y, or z in Cartesian coordinates), θ is the volumetric water content, and t is the time (Lu and Likos 2004). This equation states that the difference between the flow (flux) entering and the flow leaving a volume of soil at a point in time is equal to the change in storage of the soil volume. The change in storage for an unsaturated soil system is related to the volumetric water content, which quantifies how much water is stored in the pore space. The SWCC relates the magnitude of suction a soil system experiences with the corresponding water content.

SWCCs are typically plotted on a semi-log plot with the ordinate axis showing either saturation, gravimetric water content, or volumetric water content; the abscissa contains the matric suction in units of pressure (kPa, psf, or cm of water). Figure 1 shows an example SWCC.

Figure 1. Soil water characteristic curve (SWCC).

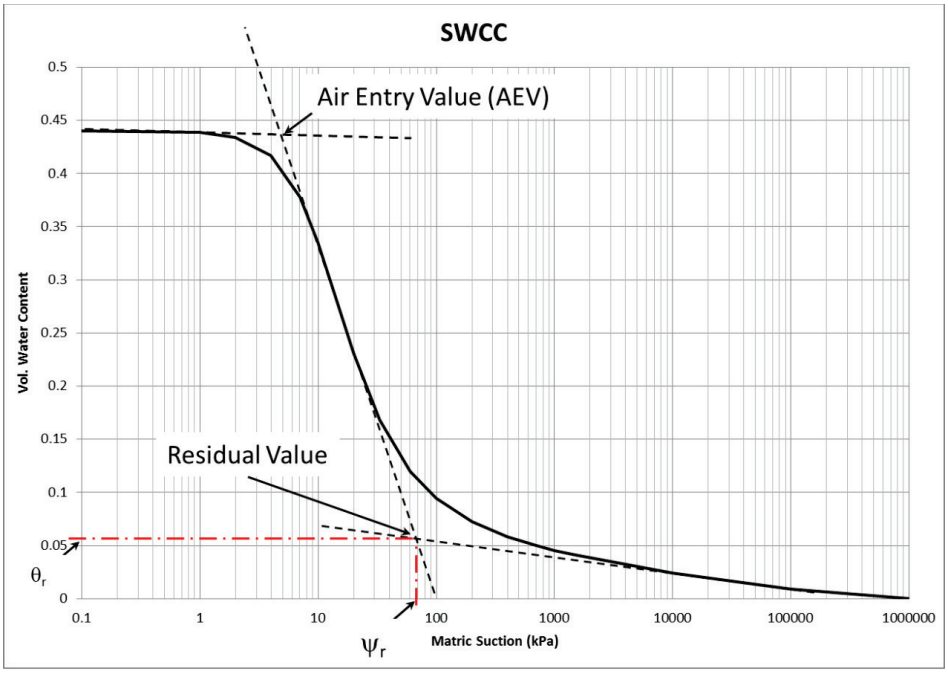

When the saturation level in a soil is less than fully saturated, negative pore water pressures develop. The term *soil suction* is defined as the negative pore water pressure. Total suction consists of two primary components: matric suction and osmotic suction (Fredlund et al. 2012). Matric suction (also known as capillary pressure) is the mathematical difference between the air and water pressures (u_a-u_w) in the soil. The air pressure is usually zero (gauge pressure), and the water pressure is negative due to surface tension. Osmotic suction is associated with both saturated and unsaturated soils and is related to the salt content in the pore water. If the salt concentration in the pore fluid changes, there is a corresponding change in the volume and shear strength of the soil (Fredlund et al. 2012). For the purpose of this report, osmotic suction will not be considered because it is considered to play a minor role in embankment performance when compared to the influence of matric suction.

The *air entry value (AEV)* is defined as the differential pressure between air and water that is required to cause desaturation of the largest pores. The AEV can be defined graphically as the intersection of the line tangent to the straight line portion of the SWCC and a horizontal line through the saturated water content. The intersection point of these two lines is the matric suction AEV. The residual water content is the point at high suctions at which very little water is retained and at which pore water is generally in the form of thin films surrounding the surface of soil grains

(Lu and Likos 2004). The *residual point* can be defined as the intersection of a tangent line along the SWCC where the curve starts to drop linearly in the high suction range (Fredlund and Xing 1994) and the tangent line used for determining the AEV. The AEV and the residual point (ψ_r,θ_r) are shown in Figure 1. Some fine-grained soil water curves do not exhibit a residual suction point. Typically, a value between 1500 to 3000 kPa is an appropriate approximation (Fredlund and Xing 1994).

One of the more common methods of fitting SWCCs to laboratory data is the equation proposed by van Genuchten (1980) shown in Equation 2.

$$\theta = \theta_r + \frac{\theta_s - \theta_r}{\left[1 + \left(\frac{\psi}{a}\right)^n\right]^m} \tag{2}$$

where θ_s and θ_r are the saturated and residual volumetric water contents; ψ is the matric suction; and a, n and m are curve-fitting parameters. The parameter m is often approximated as $(1\text{-}1/n)$. Van Genuchten (1980) gives a detailed explanation of the derivation of the fitting parameters. The van Genuchten equation is used to represent the SWCC analytically; the result can then be used to define the hydraulic conductivity function (HCF) (van Genuchten 1980).

The SWCC exhibits hysteresis as a soil cycles through wetting and drying processes. A soil undergoing a drying process will typically have a larger water content than a soil undergoing a wetting process at the same value of matric suction. Figure 2 shows an example of the wetting and drying curves.

Typically when an SWCC is obtained in the laboratory, the drying curve is measured. With regard to dams and levees, the process being modeled is undergoing a wetting process (i.e., the modeling of a flood load on an embankment). One way to address this discrepancy is to simply accept the error and use the drying curve for both wetting and drying processes. Another approach is to scale the SWCC fitting parameters to transform a drying curve into a wetting curve. Likos et al. (2013) performed a study over a wide range of soil types to assess which scaling factors were appropriate to adjust a drying curve to a wetting curve. That study found the following conversions to be appropriate:

$$\alpha^w = 2\alpha^d \tag{3}$$

$$n^w = n^d \tag{4}$$

$$\theta_s^w = \theta_s^d \tag{5}$$

where α and n are fitting parameters used in the van Genuchten SWCC fitting model, θ_s is the saturated volumetric water content, and the superscripts w and d denote wetting and drying respectively. The van Genuchten equation is shown in Equation 5.

Figure 2. Wetting and drying SWCC (data from Li et al. 2005).

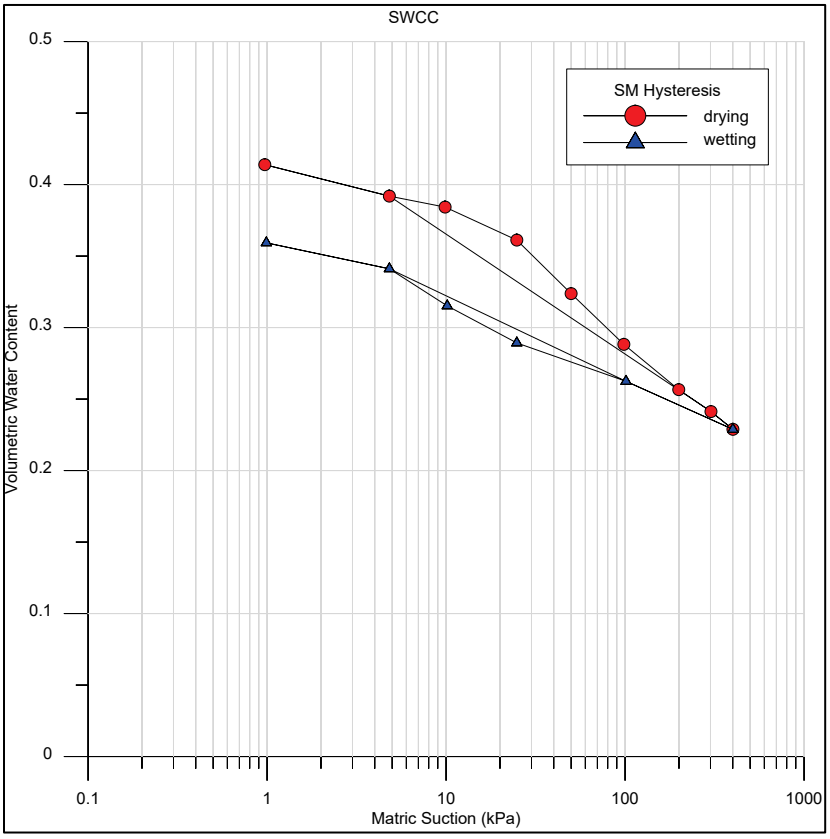

3 SWCC Prediction Methods

Two prediction methods are already incorporated into Seep/W. These are referred to in Seep/W as the Modified Kovacs method and the sample functions based on soil type. For further discussion of these two methods, it is recommended that the Seep/W user's manual be reviewed. The manual includes two closed form options as well: (1) the van Genuchten and (2) the Fredlund and Xing methods. The five methods discussed below are investigated to supplement those methods already included in the program.

Method 1: (Zapata et al. 2000)

This procedure uses the Fredlund and Xing (1994) equation (see Seep/W user's manual closed form option 1). The parameters a, b, c, and h_r are correlated to percent finer than the #200 sieve (0.074 mm) and PI (plasticity index) for plastic soils (PI>0) or D_{60} for nonplastic soils. A parameter *wPI* (defined in Equation 25) is used to derive *a*, *b*, *c*, and h_r parameters for plastic soils (PI>0).

$$wPI = P_{200} * PI \tag{6}$$

where P_{200} is the percentage of material passing the #200 sieve, expressed as a decimal, and *PI* is the plasticity index, expressed as a percentage. The parameters for plastic soils (PI>0) are defined in Equations 7 to 10:

$$a = 0.00364(wPI)^{3.35} + 4(wPI) + 11 \tag{7}$$

$$\frac{b}{c} = -2.313(wPI)^{0.14} + 5 \tag{8}$$

$$c = 0.0514(wPI)^{0.465} + 0.5 \tag{9}$$

$$\frac{h_r}{a} = 32.44e^{0.0186(wPI)} \tag{10}$$

The parameters for granular soils (PI=0) are defined in Equations 11 to 14:

$$a = 0.8627(D_{60})^{-0.751} \tag{11}$$

$$\bar{b} = 7.5 \tag{12}$$

$$c = 0.1772 \ln\left(D_{60}\right) + 0.7734 \tag{13}$$

$$\frac{h_r}{a} = \frac{1}{D_{60} + 9.7e^{-4}} \tag{14}$$

where D_{60} is the grain size at which 60% of the material is finer and $\bar{b}$ is the average value of the fitting parameter b. This method was derived from measurements on 190 soils. The samples consisted of 70 plastic soils (PI>0) and 120 nonplastic soils (PI=0). This method was included in the analysis because the input parameters are common index properties used to classify soils according to the Unified Soil Classification System (USCS), making the method easily applicable in practice.

Method 2: (Perera et al. 2005)

This method is an update of Method 1. This method defines a plastic soil as a soil that has a wPI greater than or equal to 1.0. The parameters were derived from multiple regressions correlating grain size distribution data and index properties. The Fredlund and Xing (1994) parameters are defined in Equations 15 through 25 for nonplastic soils:

$$a_f = 1.14a - 0.5 \tag{15}$$

where:

$$a = -2.79 - 14.1 \log\left(D_{20}\right) - 1.9\left(10^{-6}\right)\left(P_{200}\right)^{4.34} + 7 \log\left(D_{30}\right) + 0.055 D_{100} \tag{16}$$

$$\mathrm{D}_{100} = 10^{\left[\frac{40}{\mathrm{m}_1} + \log\left(\mathrm{D}_{60}\right)\right]} \tag{17}$$

$$m_1 = \frac{30}{\left[\log\left(\frac{D_{90}}{D_{60}}\right)\right]} \tag{18}$$

$$b_f = 0.936b - 3.8 \tag{19}$$

where:

$$b = \left\{ 5.39 - 0.29 \ln\left[P_{200} \left(\frac{D_{90}}{D_{10}} \right) \right] + 3 D_0^{0.57} + 0.021 \left(P_{200} \right)^{1.19} \right\} m_1^{0.1} \quad (20)$$

$$D_o = 10^{\left[\frac{-30}{m_2} + \log\left(D_{30} \right) \right]} \quad (21)$$

$$m_2 = \frac{20}{\log\left(\frac{D_{30}}{D_{10}} \right)} \quad (22)$$

$$c_f = 0.26 e^{0.758c} + 1.4 D_{10} \quad (23)$$

where:

$$c = \log\left(\left(m_2 \right)^{1.15} \right) - \left(1 - \frac{1}{b_f} \right) \quad (24)$$

$$h_{rf} = 100 \quad (25)$$

where D_x is the grain size diameter corresponding to x percent of the material being finer. The parameters for plastic soils ($wPI \geq 1.0$) are defined in Equations 26 through 30:

$$a_f = 32.835 \left\{ \ln\left(wPI \right) \right\} + 32.438 \quad (26)$$

$$b_f = 1.421 \left(wPI \right)^{-0.3185} \quad (27)$$

$$c_f = -0.2154 \left\{ \ln\left(wPI \right) \right\} + 0.7145 \quad (28)$$

$$h_{rf} = 500 \quad (29)$$

where:

$$wPI = P_{200} * PI \quad (30)$$

where P_{200} is the percent passing the #200 sieve (0.074 mm), expressed as a decimal, and *PI* is the plasticity index, expressed as a percentage. There were 154 nonplastic and 63 plastic soils used in the regression analysis. This method was included because the parameters are dependent on soil properties used in the USCS and because a relatively large number of samples were used to derive them.

Method 3: (Sleep 2011)

This technique uses trends among the SWCCs for different soil types in order to predict the most likely SWCC. The Unsaturated Soil Data Hydraulic Database (UNSODA), compiled and distributed by the United States Department of Agriculture (USDA), was used to create SWCC charts based on soil type. The UNSODA is based on the textural classification system; therefore, it does not contain soil index properties common in geotechnical practice. In order to relate the textural and the USCS, the SWCC data were separated by hydraulic conductivity and classified using the saturated hydraulic conductivity. Soil classifications according to saturated hydraulic conductivity (k_{sat}) are shown in Table 1.

Table 1. Soil classification based on hydraulic conductivity (Terzaghi 1996).

Soil Category	k_{sat} (cm/s)
Coarse Sand	$>10^{-1}$
Fine Sand	10^{-1} - 10^{-3}
Silty Sand	10^{-3} - 10^{-5}
Silt	10^{-5} – 10^{-7}
Clay	$<10^{-7}$

The method involves the following steps (Sleep 2011):

1. Obtain the saturated hydraulic conductivity of the soil.
2. Use the saturated hydraulic conductivity value to select the appropriate range of values from the provided figures (Table 2 presents the figures in tabular form).
3. Select the appropriate SWCC based on whether the soil is wetting or drying.

Table 2. SWCC data used to estimate appropriate curve (Sleep 2011).

k_{sat} (cm/s) Range	S	Soil Suction (kPa)				Soil Category
		Average Drying	Average Wetting	Wetting Boundary (90% conf.)	Drying Boundary (90% conf.)	
10 to 1.0E-01	1	0.7	0.1	0.009	8	Coarse Sand
	0.1	4	0.6	0.05	13.5	
1.0E-1 to 1.0E-3	1	4	0.8	0.15	30	Fine Sand
	0.1	150	25	3.5	85	
1.0E-3 to 1.0E-5	1	4.5	0.95	0.19	25	Silty Sand
	0.1	4500	1000	200	28000	
1.0E-5 to 1.0E-7	1	6	0.9	0.09	70	Silt
	0.14	X	X	100000	X	
	0.28	X	100000	X	X	
	0.4	100000	X	X	X	
	0.55	X	X	X	100000	

4. Input the two point values into Seep/W, Data Point Function, by using Equation 31 or 32 to convert saturation to volumetric water content:

$$\theta_{100\%} = n_p \tag{31}$$

$$\theta_{10\%} = n_p * S_{10\%} \tag{32}$$

where θ is the volumetric water content, n_p is the porosity, and S is saturation.

5. Repeat steps 1-4 to obtain any other curves deemed necessary.

Figure 3 shows how the curves would look for coarse sand following the process outlined above. The wetting and drying boundaries are based on a 90% confidence interval. The wetting curve was constructed based on an approximation that the wetting curve is usually one order of magnitude smaller than the drying curve. Sleep (2011) provides a more complete discussion on the formulation of the method.

Figure 3. SWCC for coarse sand, n=0.35, Sleep (2011).

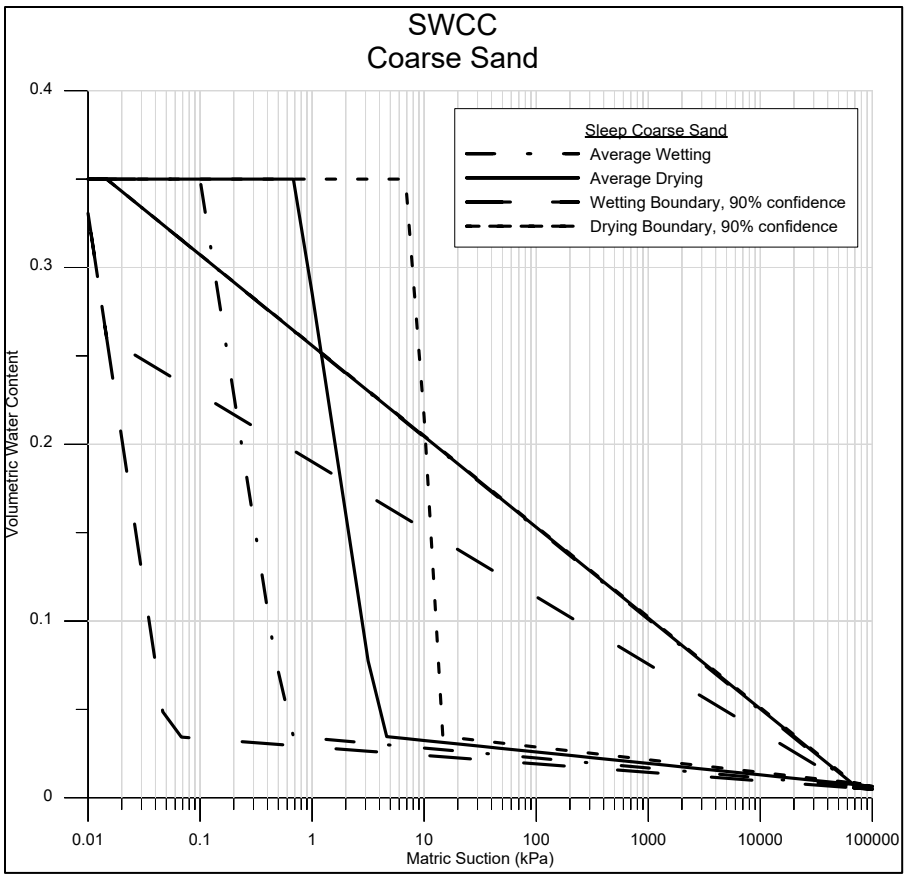

The limitation of this procedure is that there is no method to predict the SWCC for clay materials. This method was selected for comparison because it is easy to use and it provides the upper and lower bound SWCCs for use in sensitivity analyses.

Method 4: (Tomasella and Hodnett 1998)

This method uses a pedotransfer function (PTF) to derive the SWCC. This method was derived for use with soils from the Brazilian Amazon using 1,162 soils from the region. The Brooks and Corey model was used to model the SWCC, and the coefficients were derived using grain size according to the textural classification system. Equation 33 shows the Brooks and Corey model.

$$\theta = \begin{cases} \theta_r + (\theta_s - \theta_r)\left(\frac{\psi B}{\psi}\right)^{\frac{1}{B}} & -\infty < \psi \le \psi_B \\ \theta_s & 0 > \psi > \psi_B \end{cases} \tag{33}$$

where θ is the volumetric water content, ψ is the matric potential (kPa), the subscripts *r* and *s* respectively denote residual and saturated water contents, $1/B$ is an empirical constant, and ψ_B is the matric potential (kPa) corresponding to the air entry pressure. For this method, the Brooks and Corey parameters are estimated solely from the grain size distribution using Equations 34 to 37:

$$\psi_B = 0.285 + 7.33\left(10^{-4}\right)P_{si}^{\ 2} - 1.3\left(10^{-4}\right)P_{si} * P_{cl} + 3.6\left(10^{-6}\right)P_{si}^{\ 2}P_{cl} \quad (34)$$

$$B = e^{\left(1.197 + 4.17\left(10^{-3}\right)P_{si} - 4.5\left(10^{-3}\right)P_{cl} + 8.94\left(10^{-4}\right)P_{si}P_{cl} - 1.0\left(10^{-5}\right)P_{si}^{\ 2}P_{cl}\right)} \quad (35)$$

$$\theta_s = 40.61 + 0.165P_{si} + 0.162P_{cl} + 1.37\left(10^{-3}\right)P_{si}^{\ 2} + 1.8\left(10^{-5}\right)P_{si}^{\ 2}P_{cl} \quad (36)$$

$$\theta_r = -2.094 + 0.047P_{si} + 0.431P_{cl} - 8.27\left(10^{-3}\right)P_{si}P_{cl} \quad (37)$$

where P_{si} is the percent silt and P_{cl} is the percent clay. Some ranges of material type may produce a small negative value for θ_r; in these cases, θ_r should be assigned a value of 0. This method was intended for use with tropical fine-grained soils and is based on the textural classification system.

Method 5: (Rawls et al. 1991)

This method is based on previous work by Rawls et al. (1982) in which a regression analysis was performed on existing SWCC data to derive the Brooks and Corey SWCC parameters; the Brooks and Corey model is defined in Equation 33. The equations for the Brooks and Corey parameters resulting from the regression analyses are

$$\psi_B = e^{\begin{bmatrix} 5.33967 + 0.1845P_{cl} - 2.4839n_p - 0.00214P_{cl}^{\ 2} - 0.04356P_{sa}n_p - 0.61745P_{cl}n_p \\ +0.001436P_{sa}^{\ 2}n_p^{\ 2} - 0.008554P_{sa}^{\ 2}n_p^{\ 2} - 0.00001282P_{sa}^{\ 2}P_{cl} + 0.008954P_{sa}^{\ 2}n_p \\ -0.0007247P_{sa}^{\ 2}n_p + 0.0000054P_{cl}^{\ 2}P_{sa} + 0.5n_p^{\ 2}P_{cl} \end{bmatrix}} \quad (38)$$

$$\lambda = e^{\begin{bmatrix} -0.784 + 0.0177P_{sa} - 1.062n_p - 0.000053P_{sa}^{\ 2} - 0.00273P_{cl}^{\ 2} + 1.111n_p^{\ 2} - 0.03088P_{sa}n_p \\ 0.000266P_{sa}^{\ 2}n_p^{\ 2} - 0.0061P_{cl}^{\ 2}n_p^{\ 2} - 0.00000235P_{sa}^{\ 2}P_{cl} + 0.007987P_{cl}^{\ 2}n_p - 0.00674n_p^{\ 2}P_{cl} \end{bmatrix}} \quad (39)$$

$$\begin{aligned} \theta_r = &-0.0182 + 0.000873P_{sa} + 0.005135P_{cl} + 0.02939n_p - 0.000154P_{cl}^{\ 2} \\ &-0.00108P_{sa}n_p - 0.000182P_{cl}^{\ 2}n_p^{\ 2} + 0.000307P_{cl}^{\ 2}n_p - 0.00236n_p^{\ 2}P_{cl} \end{aligned} \quad (40)$$

where P_{sa} is percent sand, P_{cl} is percent clay, and n_p is the porosity. The bubbling pressure, otherwise known as the air entry value, $\psi_{B,}$ is in centimeters of water; λ is the pore size index (λ=1/B); and θ_r is the residual water content. These equations (Equations 38-40) are reported to be valid for 5%<P_{Sa}<70% and 5%<P_{cl}<60%.

4 Evaluation of Prediction Methods

An evaluation of the prediction methods was performed by comparing laboratory-measured SWCCs obtained from the literature for four soil types to the curves predicted by the five methods above. This evaluation was conducted to illustrate how the prediction methods compared across a range of soil types. By using independent data (data not included in the method development), the performance of the prediction methods was also evaluated. The predicted SWCCs obtained from each method for the four soils were also carried through a simple transient seepage analysis to quantify the influence of the differences in SWCC in terms of the time required for a wetting front to propagate. Table 3 shows the soils used, classified according to the USCS, and each reference from which the data were obtained.

Table 3. SWCC soil data set.

USCS	Reference
ML	Askerinejad et al. 2011
SM	Li et al. 2005
CH	Tinjum et al. 1997
SP	Song et al. 2012

Table 4 shows the material properties necessary to predict the SWCC using each of the five prediction methods. The CH sample was compacted at optimum water to maximum dry density by the modified Proctor method.

Table 4. Material properties of the soil data set.

USCS	D_{10} (mm)	D_{20} (mm)	D_{30} (mm)	D_{60} (mm)	D_{90} (mm)	%Sand	%Silt	%Clay	%Passing #200 *	LL	PL	PI	Porosity	k_{sat} (cm/s)
ML	0.0075	0.06	0.085	0.28	0.53	78.87	16.45	3.55	0.27	31	20	11	0.46	1.00E-05
SM	0.0019	0.013	0.045	0.59	2.6	53	20	12	0.35	57	40	17	0.43	1.00E-04
CH	-	-	-	-	-	6	41	53	0.94	67	21	46	0.345	1.00E-09
SP	0.43	0.47	0.5	0.6	0.75	100	0	0	0	NP			0.42	1.00E-01

*Expressed as a decimal, necessary for Zapata et al. (2000) and Perera et al. (2005) methods.

Comparison of the Prediction Methods

The predicted SWCCs obtained from each method for the soils in Table 4 were graphically compared to the laboratory-measured curve obtained

from the literature. These analyses were performed on a very limited dataset (four samples), making only general observations regarding the predictive methods possible. All of the sample SWCCs were drying curves. Figure 4 shows the various predicted SWCCs and the laboratory-measured curve for the ML material.

Figure 4. Predicted and laboratory SWCC for ML material.

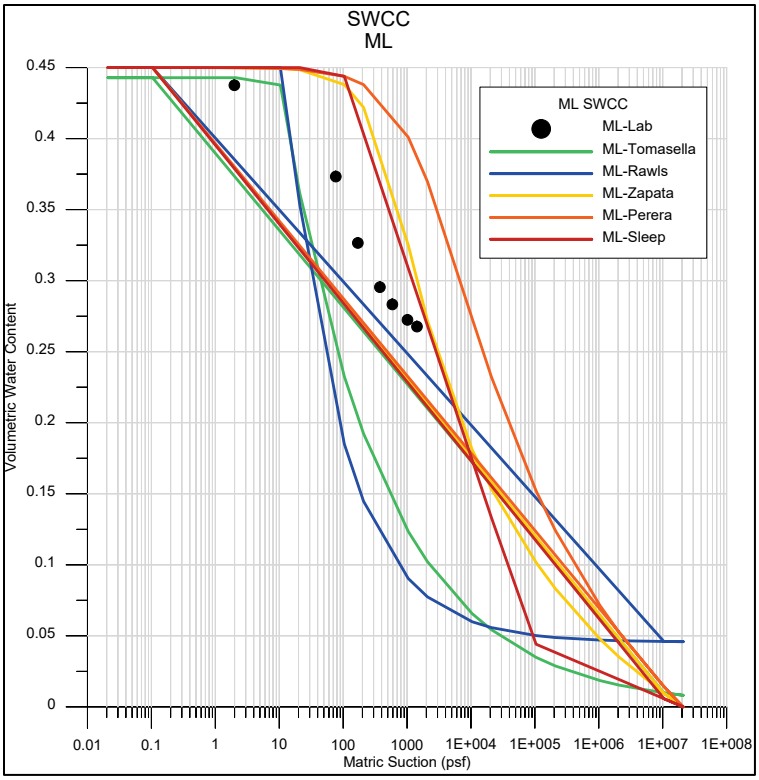

The closest approximation of the laboratory measured SWCC for the ML material was obtained using Sleep's method (2011). However, the measured data are slightly concave with respect to the vertical axis, and the two methods outlined by Rawls et al. (1991) and Tomasella and Hodnett (1998) seem to approximate this shape the best.

Figure 5 shows the predicted and laboratory SWCC for the compacted CH. Tomasella and Hodnett's method (1998) overpredicts the SWCC by a large margin. This overprediction is likely due to the reliance of this method on predicting the saturated volumetric water content while the other methods rely on user input of the saturated volumetric water content (estimated as porosity). For this sample the closest approximation of the laboratory-measured SWCC data was acquired by Sleep's method (2011), which uses the silt curve due to the absence of a clay curve for this method.

Figure 5. Predicted and laboratory SWCC for compacted CH.

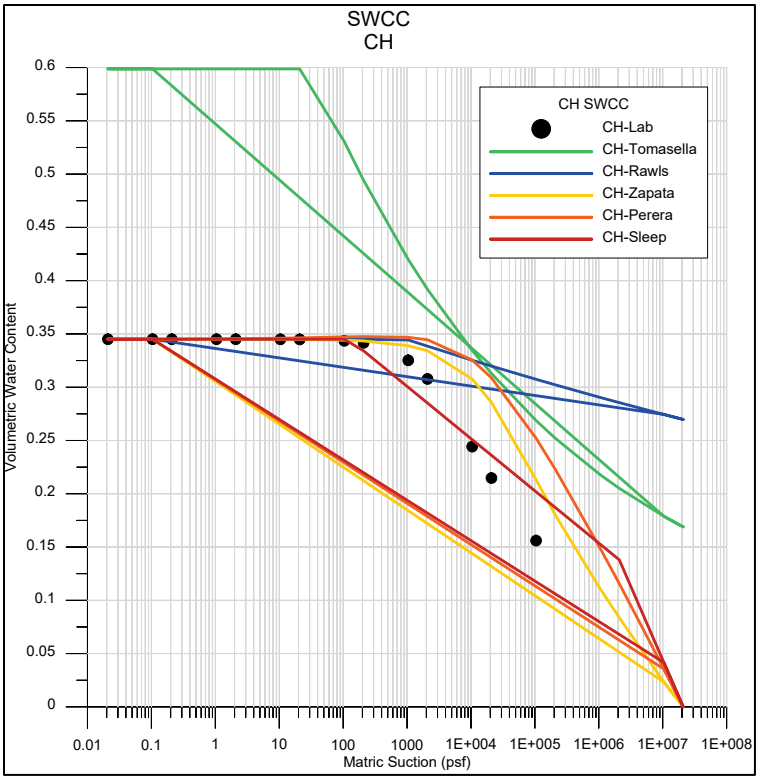

Figure 6 shows the predicted and the laboratory-measured SWCCs for the SM sample. The measured SWCC data are convex with regard to the vertical axis. This shape is matched accurately by the Brooks and Corey function utilized by Tomasella and Hodnett (1998) and Rawls et al. (1991). The closest approximation of the laboratory data with regard to shape and accuracy was obtained by Zapata et al. (2000).

Figure 7 shows the predicted and laboratory SWCC for the SP material. The shape of the measured SWCC is nearly vertical after it reaches the AEV, occurring at approximately 35 kPa. Zapata et al.'s (2000) method most nearly approximates the measured SWCC data in shape and accuracy.

Considering the limited data set (four samples) analyzed, Zapata et al.'s (2000) and Sleep's (2011) methods seem to approximate more accurately the measured SWCC with regard to both shape and accuracy across the range of soils.

Figure 6. Predicted and laboratory SWCC for SM material.

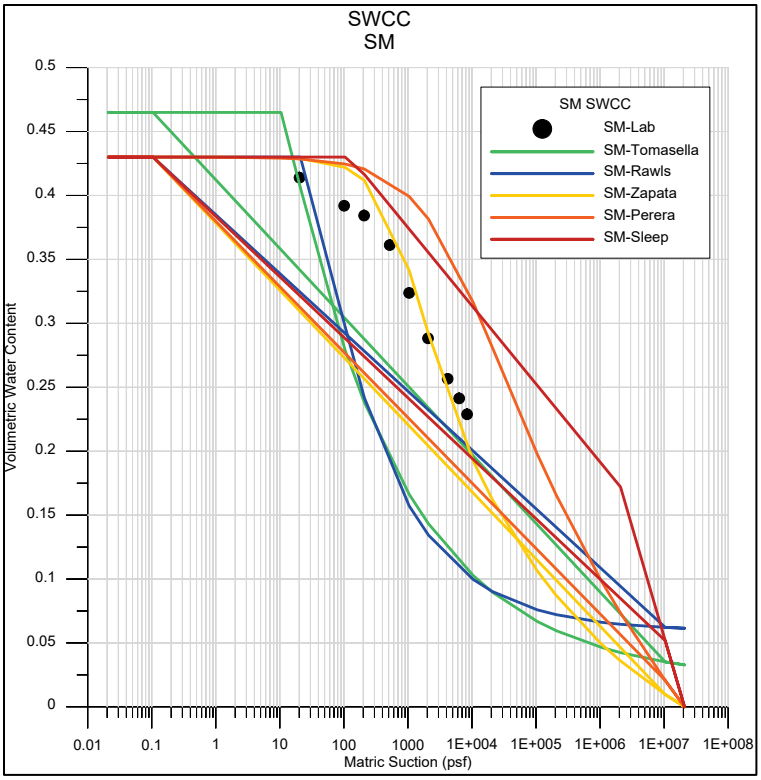

Figure 7. Predicted and laboratory SWCC for SP material.

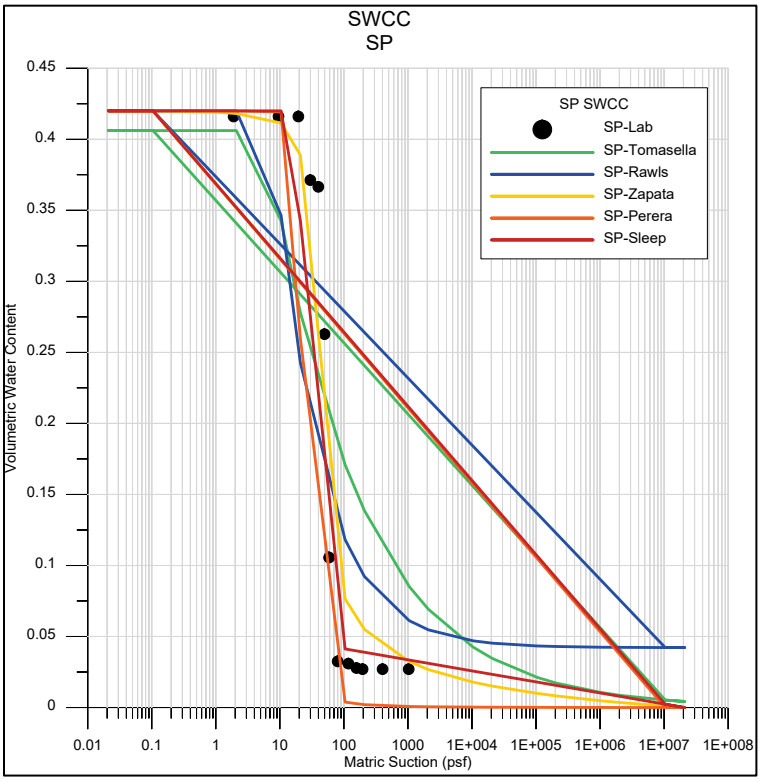

Impacts of SWCC Prediction Error on Transient Seepage Analyses

The second analysis was conducted to illustrate how the error associated with each respective prediction method impacts the results of a transient seepage analysis. The analysis was conducted by using the finite element software Seep/W (2007) along with the SWCC prediction Add-In developed for this study. The problem geometry will be briefly summarized below; Tracy et al. (2015) gives a more detailed definition of the problem. The problem consists of a column 10 ft wide and 50 ft tall. The grid size is 2 ft by 2 ft, and the time step is set to 0.001 days (86.4 s). Figure 8 shows the column geometry and total head boundary conditions. The model was set to an arbitrary nearly dry state (h_t = -30 ft), and at time greater than zero the total head at the upper boundary was set to 50 ft. This simulates infiltration from the upper surface of the column, similar to the Green-Ampt infiltration problem, as defined in Tracy et al. (2016).

Figure 8. Finite element mesh with boundary conditions.

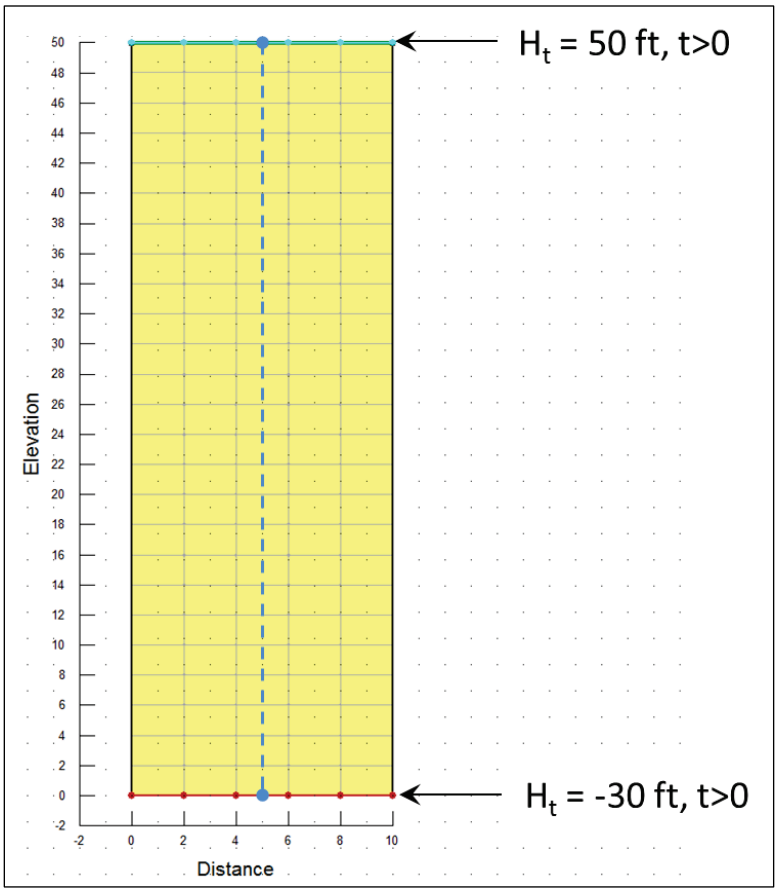

The SWCC developed for each of the samples shown in Table 4 and Figures 4-8 was used in this analysis. The process modeled was a wetting process, and all of the SWCCs were drying curves; but for comparison purposes, these SWCCs were used with no adjustment. The hydraulic conductivity ratio was assumed to be 1, and the van Genuchten hydraulic conductivity function (1980) was used. Each analysis was run for a simulated five days; and at the end of the simulated time, the total heads were collected from the nodes that lie along the dashed line shown in Figure 8.

Figure 9 shows the total head contours for the laboratory-measured ML SWCC. The infiltration wetting front had not advanced more than a foot after five days. This was typical for all of the analysis. Of interest for this particular analysis was how each of the predicted SWCCs compared to the laboratory-measured SWCC in terms of loading response. Figures 10 through 13 show the profiles of pressure head values for each prediction method and the laboratory-measured SWCC for each soil.

The results shown in Figure 10 show that the SWCC predicted by the Rawls et al. method (1991) closely matched the results of the laboratory SWCC. This is interesting because, even though the Rawls method (as well as the Tomasella method [Tomasella and Hodnett 1998]) matched the shape of the lab SWCC, they were rather inaccurate. An investigation of the hydraulic conductivity functions (HCF) (Figure 14) shows the Rawls et al. method (1991) more closely matches the laboratory-measured SWCC HCF.

Figures 11 and 12 show that all prediction methods matched the laboratory data more closely for the SM and CH soils than for the ML material. In the case of the CH material, this is in part due to the limited development of the wetting front over the period of five days. Table 5 shows the mean squared error (MSE), which is a measure of the difference between the pore pressures modeled using the laboratory-measured SWCC and the pore pressures obtained using the various predicted SWCCs. Equation 42 shows how the MSE was calculated:

$$MSE = \frac{1}{n}\sum_{i=1}^{n}\left(\hat{Y}_i - Y_i\right)^2 \tag{42}$$

where n is the quantity of data points; for this case there were 26 data points, one for each node. Y_i is the total head values obtained at the 26 different nodes for the analysis that used the predicted SWCC, and $\hat{Y}_i$ is

the total head values from the laboratory-measured SWCC analysis. The smaller the MSE value, the more accurately the results of the predicted SWCC analysis matched the results of the analysis performed using the laboratory-measured SWCC. The MSE values for the compacted CH are all less than ten, but Sleep's (2011) and Tomasella and Hodnett's (1998) methods were much smaller than one, indicating that these two prediction methods closely matched the results of the laboratory-measured SWCC analysis. This is an interesting result, considering that Sleep's (2011) prediction was derived from the silt data as a result of no clay SWCC curve's being available in the UNSODA database (Nemes et al. 2001). Tomasella and Hodnett's (1998) method was derived from mainly fine-grained soil, so its adequate prediction of the clay SWCC should be expected.

Figure 9. Total head contours, laboratory-measured ML SWCC.

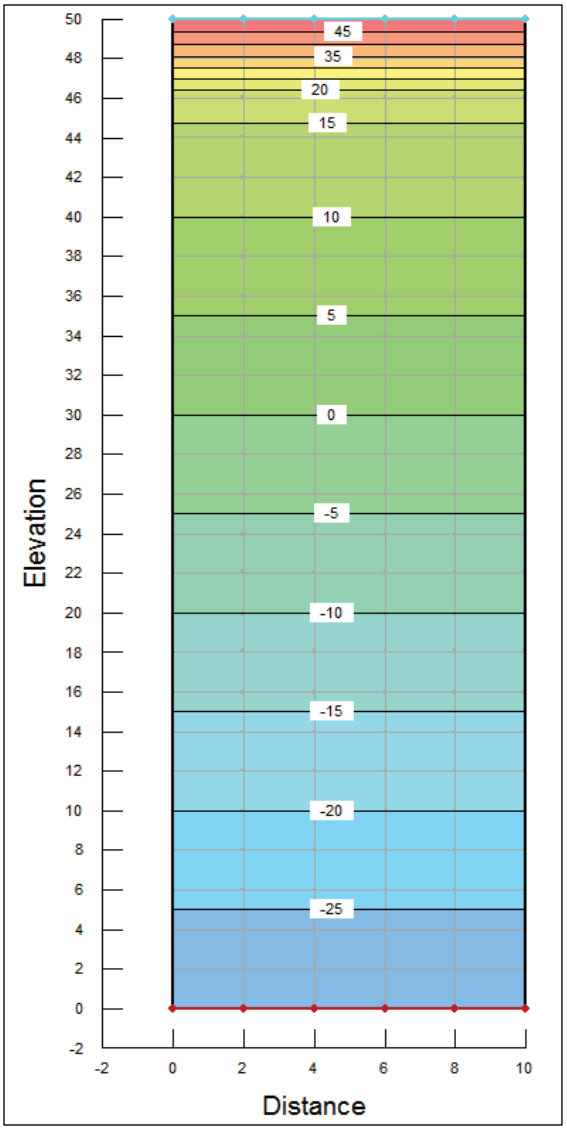

Figure 10. Profile of pressure head values after five days for ML.

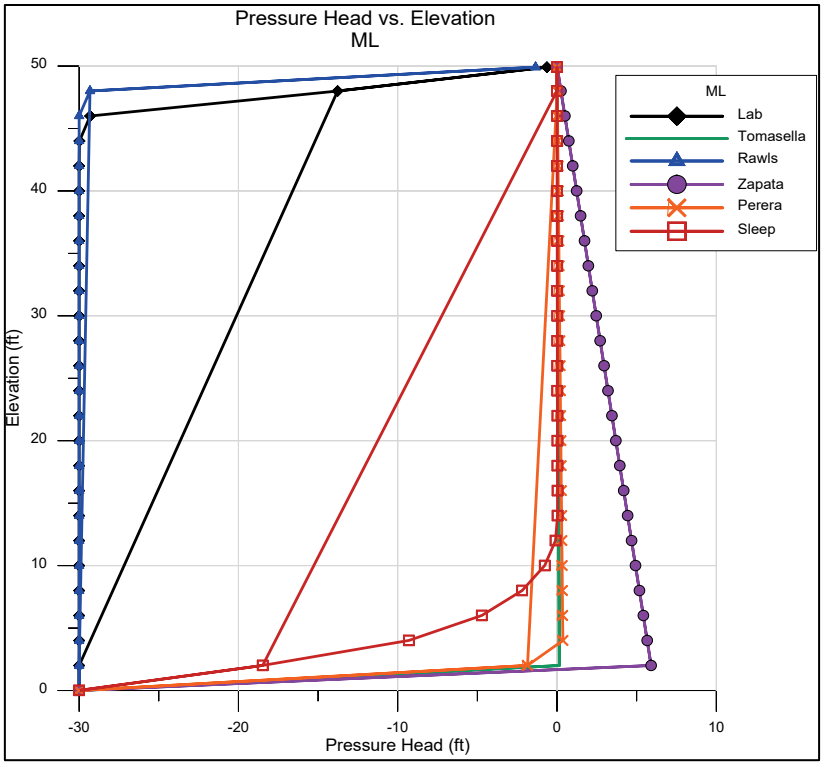

Figure 11. Profile of pressure head values after five days for compacted CH.

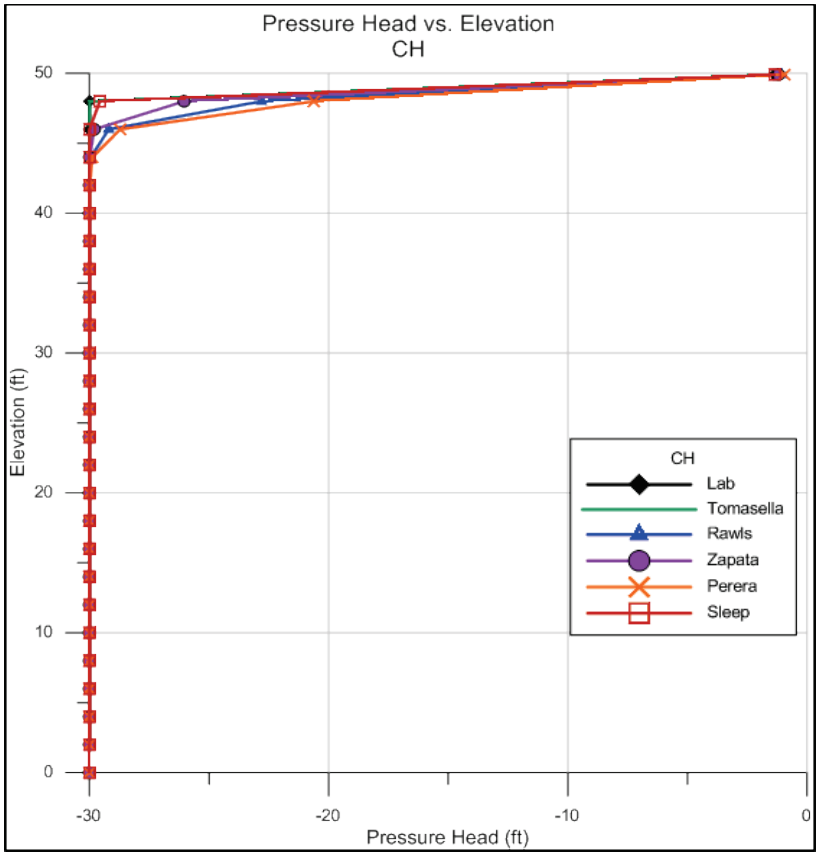

Figure 12. Profile of pressure head values after five days for SM.

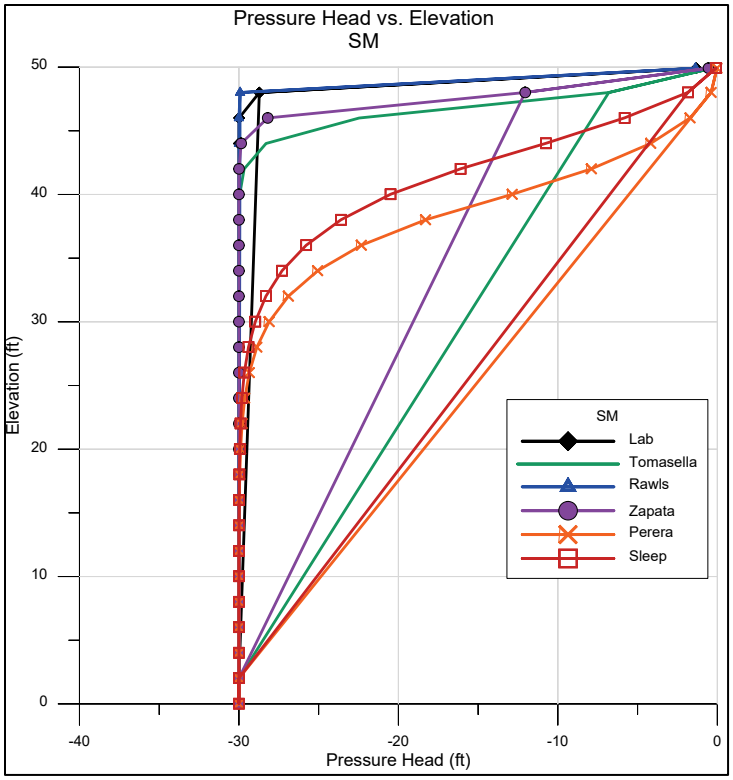

Figure 13. Profile of pressure head values after five days for SP.

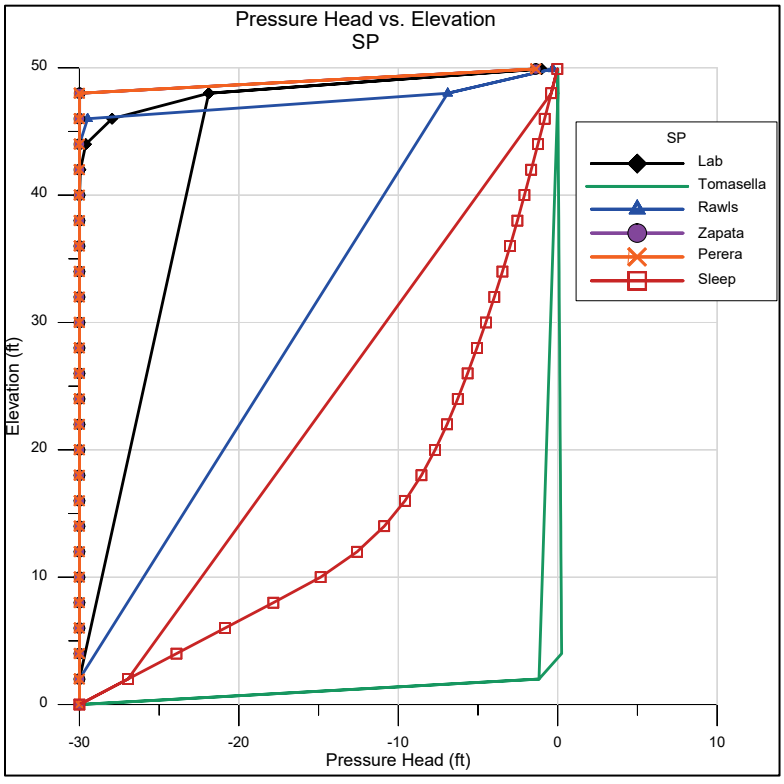

Figure 14. Hydraulic conductivity function for ML.

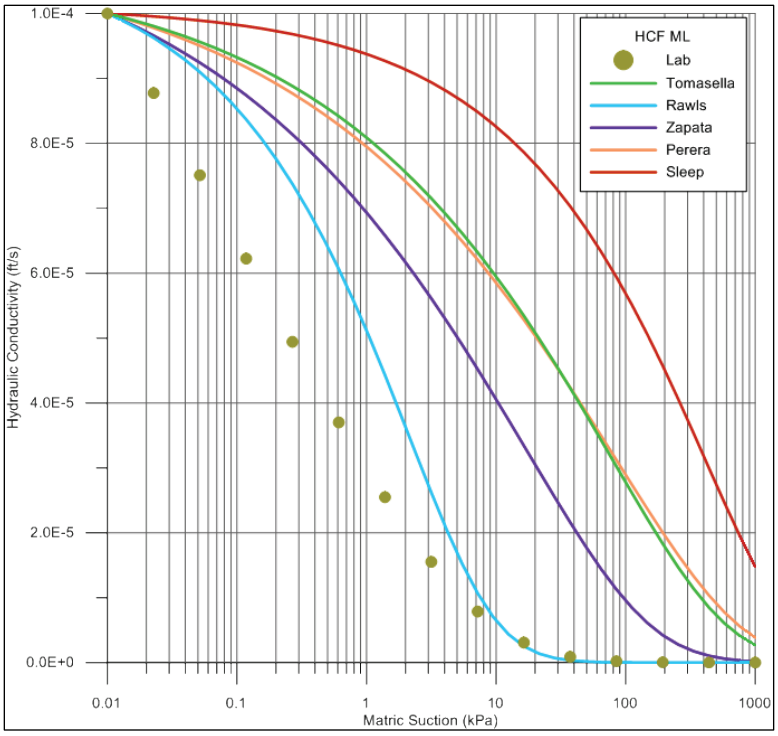

Table 5. Results of transient seepage analysis MSE between predicted SWCC and laboratory-measured SWCC.

Material	Tomasella and Hodnett	Rawls	Zapata	Perera	Sleep
ML	8.06E+02	9.34E+00	9.83E+02	8.08E+02	7.38E+02
SM	2.08E+01	5.58E-02	1.08E+01	1.27E+02	7.82E+01
CH	2.90E-06	2.02E+00	6.05E-01	3.46E+00	7.18E-03
SP	8.13E+02	8.75E+00	2.70E+00	2.71E+00	4.60E+02

Comparing the results from this rather limited analysis, Rawls et al.'s (1991) method consistently matches the laboratory-measured SWCC analysis's results. Given the size of the data set, these results are very preliminary; but each prediction method seems to give reasonable results, with the method proposed by Rawls et al. (1991) being applicable across the full range of soil types investigated, based on the pore pressure results.

Saturation Coefficient

Evaluating the relative significance of the differences in the SWCC predictions on the results of a transient seepage analysis from the above pressure profiles is rather difficult. To truly evaluate the significance of the different SWCC curves, the solution must be described over the entire time

domain. This has been done in the past either by plotting the evolution of the pore pressure at certain locations over time or by providing profiles of the pore pressure at discrete points in time (Lam and Fredlund [1984], Cedergren [1997]). Using either of these approaches for fine-grained soils is still rather inconvenient due to the sharp transition between unsaturated and saturated soils at the wetting front. As seen by plots of pressure profiles at different times for the CH column in Figure 15, the response throughout much of the sample is essentially zero until the wetting front approaches, at which point the pressure rapidly increases to a near constant value. Plotting numerous profiles or pressure versus time curves on the same plot to compare the various methods would produce a figure quite cluttered and difficult to compare. Therefore, the concept of a normalized saturation coefficient was developed to allow a continuous comparison of the transient seepage solutions for each of the predictive methods.

Figure 15. Elevation versus pressure head at different times.

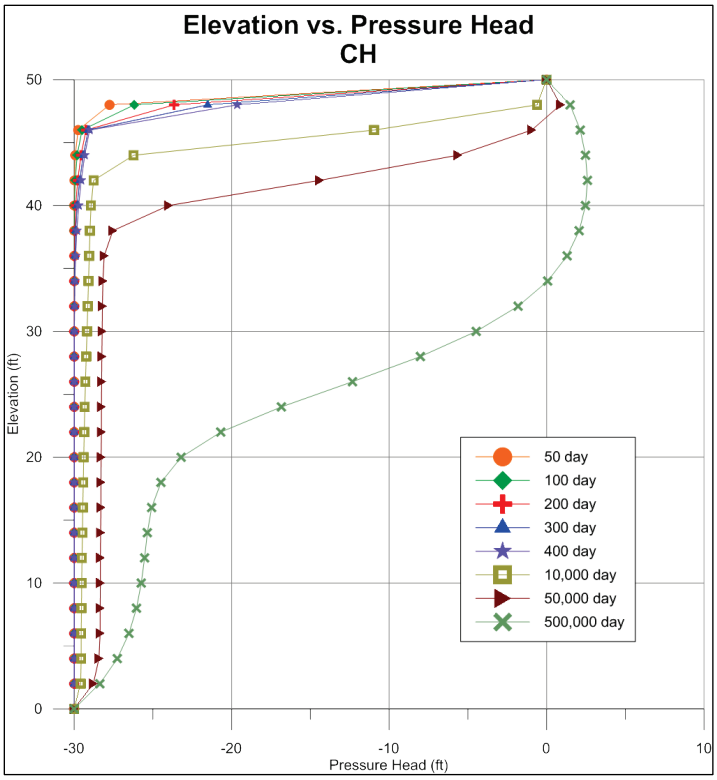

The normalized saturation coefficient (ω) is a dimensionless parameter that varies from a value of zero at time zero to a value of 1.0, corresponding to steady state seepage conditions. The normalized saturation coefficient is computed as

$$\omega = \frac{\int S_t dA - \int S_i dA}{\int S_{ss} dA - \int S_i dA} \tag{43}$$

where S_t is the saturation at time t , S_i is the saturation corresponding to the initial conditions, and S_{ss} is the saturation corresponding to the steady state seepage solution. The integrals are evaluated over the entire seepage domain of interest (the full column, in this particular case.) As seepage is a diffusion process, the change in ω over time can be thought of as an analogue to the average degree of consolidation. Just as the average degree of consolidation describes the progress towards complete consolidation, ω describes the progress a transient wetting front has made towards the steady state solution. The value of ω is the percent of available pore space (pore space that would be saturated at steady state but is initially empty) that has become saturated at any point in time. Using the concept of the normalized saturation coefficient, a more thorough evaluation of the differences in the SWCC predictions on the transient column analysis was able to be performed.

A final numerical analysis was conducted to see how the predicted SWCC and the associated prediction error impacted a numerical analysis by using the finite difference program FLAC (Fast Lagrangian Analysis of Continua). The same geometry used in the SEEP/W analysis was used in the FLAC analysis. The two-phase-flow option was used in FLAC and, with this option, only van Genuchten's (1980) fitting parameters are available for use. Not all of the SWCC prediction methods use van Genuchten's fitting equation, so each of the predicted SWCCs had to be fitted with this equation. It was recognized that some additional error might have been incorporated with this procedure, but the error was assumed to be small when compared to error already present. Figure 16 shows the SM-predicted SWCCs fitted with van Genuchten's (1980) equation (the solid line represents the predicted curve, and the dashed line represents the van Genuchten fitted curve). Zapata et al.'s (2000) and Rawls et al.'s (1991) SWCCs fit with van Genuchten's equation very well while Sleep's (2011) equation did not. The likely reason for the poor fit to Sleep's SWCC was its odd shape.

Figure 16. Comparison of predicted method and methods fitted with van Genuchten equation (1980).

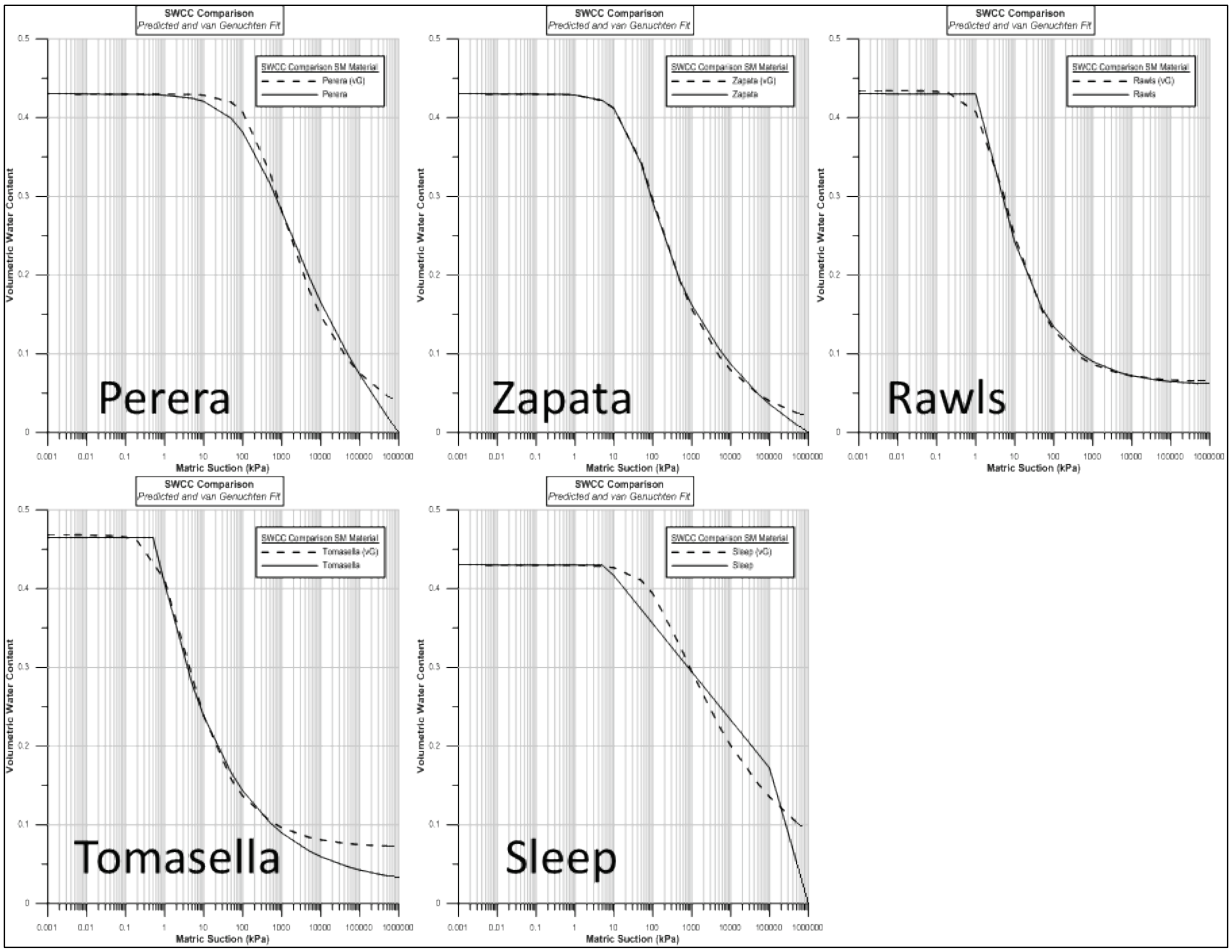

The material properties used in the FLAC analysis are presented in Table 6.

The following define the properties shown in Table 6: a, b, and c are constant parameters; and P_0 is equivalent to van Genuchten's α (1980) (a in Equation 2). The constant a is equal to van Genuchten's (1980) m, and b and c are the l parameters from the hydraulic conductivity function as shown in Schaap and Leij (2000). Instead of using hydraulic conductivity, FLAC uses the mobility coefficient, which is simply the ratio of the hydraulic conductivity to the unit weight of water.

Table 6. Material properties used in the FLAC analysis.

FLAC Properties								
SWCC origin	Material	Porosity	a	b	c	P_0 (psf)	S_r	κ (ft^4/lb*s)
Lab	ML	0.44	0.11	0.5	0.5	17.30	0.00	5.26E-09
Tomasella		0.45	0.26	0.5	0.5	18.51	0.02	
Rawls		0.45	0.40	0.5	0.5	23.46	0.11	
Zapata		0.45	0.22	0.5	0.5	431.00	0.00	
Perera		0.45	0.23	0.5	0.5	2089.02	0.00	
Sleep		0.45	0.27	0.5	0.5	519.61	0.00	
Lab	SM	0.41	0.16	0.5	0.5	355.05	0.00	1.60E-08
Tomasella		0.465	0.29	0.5	0.5	26.82	0.17	
Rawls		0.43	0.32	0.5	0.5	51.13	0.15	
Zapata		0.43	0.23	0.5	0.5	705.95	0.00	
Perera		0.43	0.23	0.5	0.5	5686.79	0.00	
Sleep		0.43	0.15	0.5	0.5	2437.20	0.00	
Lab	CH	0.35	0.17	0.5	0.5	2155.00	0.00	6.84E-13
Tomasella		0.60	0.12	0.5	0.5	47.81	0.14	
Rawls		0.35	0.10	0.5	0.5	1987.62	0.54	
Zapata		0.34	0.26	0.5	0.5	29246.34	0.00	
Perera		0.34	0.28	0.5	0.5	68241.47	0.00	
Sleep		0.34	0.15	0.5	0.5	2437.20	0.00	
Lab	SP	0.41	0.88	0.5	0.5	51.58	0.05	5.26E-05
Tomasella		0.41	0.26	0.5	0.5	8.89	0.01	
Rawls		0.42	0.43	0.5	0.5	11.33	0.10	
Zapata		0.42	0.64	0.5	0.5	40.48	0.03	
Perera		0.42	0.88	0.5	0.5	21.69	0.00	
Sleep		0.42	0.68	0.5	0.5	28.85	0.04	

The normalized saturation coefficient was computed at each time step in FLAC as

$$\omega = \frac{\sum S_{tn} A_n - \sum S_{in} A_n}{\sum S_{ssn} A_n - \sum S_{in} A_n} \tag{44}$$

where ω is the saturation coefficient, S is the degree of saturation for each zone, A is the zone area, and n is the number of zones in the finite difference grid. The saturation coefficient is calculated by first allowing the solution to come to equilibrium with the initial conditions applied, which are the same as described in the SEEP/W analysis. The initial saturation (S_i from

Equation 42) and the area were multiplied and summed over the entire grid, and this value was stored for later use. The next step was to apply the infiltration boundary conditions and run the analysis until steady state conditions were reached. Once steady state conditions were reached, the steady state zone saturations (S_{ss} from Equation 42) and the areas were multiplied and summed over the entire grid, and this value was stored. After these two steps were completed, the program was reset to the initial conditions and the infiltration boundary conditions were reapplied; this allowed the saturation coefficient to be calculated and plotted against flow time.

Figure 17 shows the levee saturation coefficient plotted against time for the ML material. The solid line represents the analysis using the laboratory-measured SWCC data. The results that most closely matched the analysis using the lab data were attained by the SWCCs predicted by the Rawls et al. (1991) and Tomasella and Hodnett methods. The Perera, Sleep, and Zapata methods all reached 90% of steady state much faster than the laboratory analysis did. The times to reach 90% steady state for the Perera, Sleep, and Zapata methods were 315.75, 807.87 and 873.29 days, respectively, while at 1,000 days the analysis using lab data was at a saturation coefficient value of 57.9%. From observation of Figure 17, it is readily seen that all of the predictive methods except the Tomasella and Hodnett method lead to conservative results.

Figure 17. Saturation versus time for the ML material.

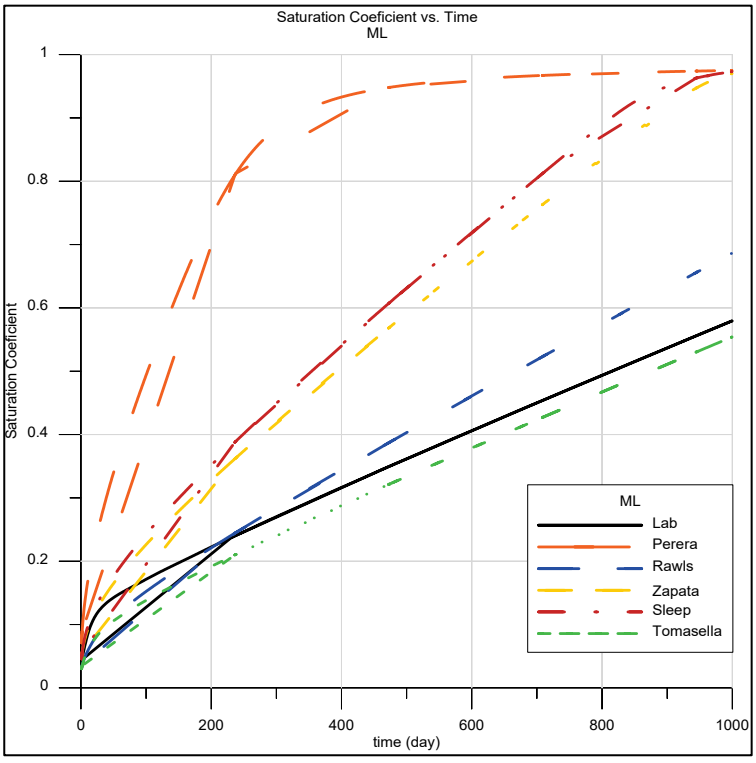

Figure 18 shows the saturation coefficient versus time for the CH material. The results of this analysis show that Sleep's (2011) method most closely approximates the results of the numerical analysis using the laboratory-measured SWCC. Tomasella's predicted SWCC leads to a solution that greatly underpredicts the wetting front when compared to the laboratory analysis. The analyses performed using Perera's, Rawls's, and Zapata's predicted SWCC overpredict the location of the wetting front. At a time of 500,000 days, the saturation coefficient for the laboratory analysis was 44.1%, while for Perera's, Rawls's and Zapata's analyses the coefficient values were 79.6%, 86.5% and 86.4% respectively. The low values for Tomasella and Hodnett's predicted SWCC are likely due to the higher-than-measured saturated volumetric water content, which is nearly double the measured value. Also, the AEV for this SWCC is extremely low compared to the other curves shown in Figure 5. Once again, all of the predictive methods except for the Tomasella and Hodnett method lead to a conservative estimate of the wetting front location.

Figure 18. Saturation versus time for the CH material.

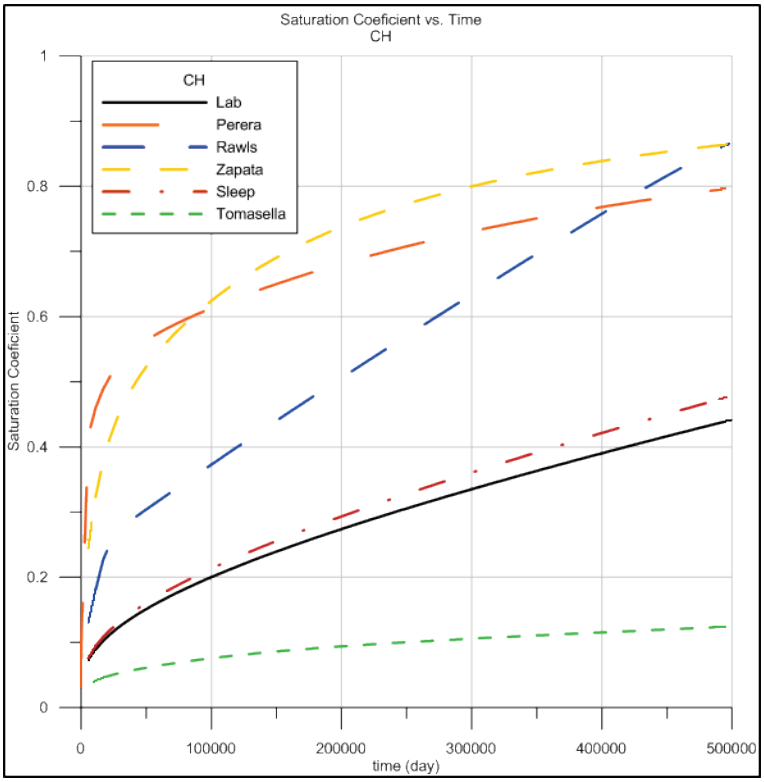

The results of the analyses performed on the SM material are presented in Figure 19. The analyses performed using Rawls' and Tomasella and Hodnett's predicted SWCC both underpredict the saturation coefficient. At

a flow time of 291.2 days, the laboratory analysis value of the saturation coefficient was at 90% while the values for Rawls' and Tomasella and Hodnett's analyses were 64% and 56%, respectively. The rest of the analyses overpredicted the saturation coefficient, with Zapata's most closely matching the laboratory results. At a flow time of 291.2 days Perera's, Sleep's, and Zapata's saturation coefficients were 98.6%, 99.6%, and 99%, respectively.

Figure 19. Saturation versus time for the SM material.

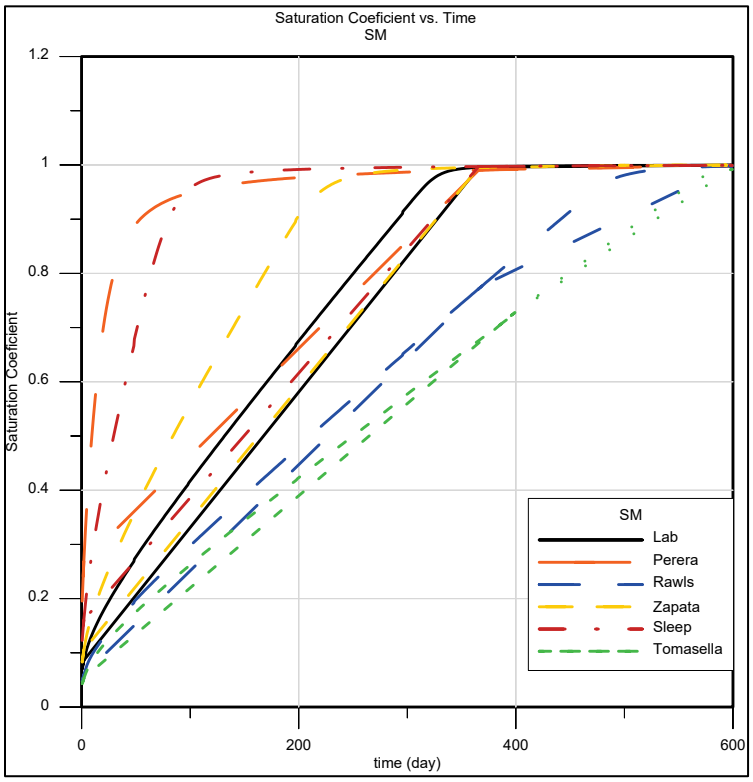

The saturation coefficient versus time obtained for analysis of the SP material is shown in Figure 20. The results of these analyses show that Perera's method matches the analysis using the laboratory data the best. An MSE of 6.18E-4 was calculated for Perera's predicted SWCC compared to an MSE of 0.275, the poorest fit, by Tomasella's predicted SWCC. A saturation coefficient of 90% occurred for the laboratory analysis at 43.2 min, while at this same time the saturation coefficients for Rawls, Sleep, Tomasella and Zapata were 23.6%, 63.9%, 24.6%, and 57.1%, respectively. It should be noted that all predictive methods yielded non-conservative results for the SP soil.

Figure 20. Saturation versus time for the SP material.

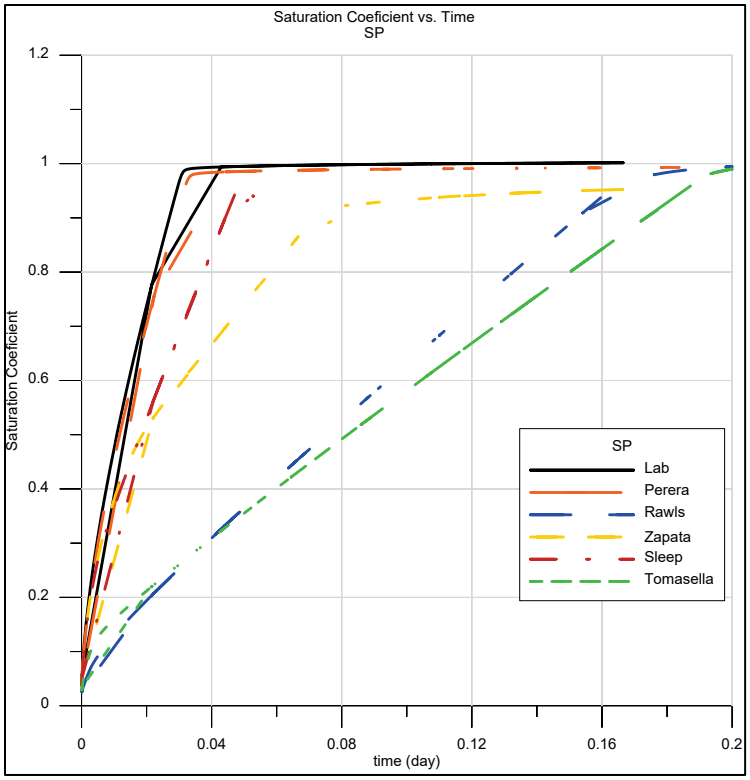

The results of this analysis showed that the normalized saturation coefficient provides a useful way to characterize the results of a transient analysis. Portraying the transient solutions in terms of ω allowed the entire transient seepage process to be represented by a single numeric value such that the transient solutions from using the various SWCC predictive methods could readily be compared on a single graph. The results show that the Rawls method of predicting the SWCC performed well for the ML and SM materials but not for the SP and CH materials. While Sleep's method closely matched the laboratory CH and SP results, it did not perform as well with the silty materials. The use of ω not only evaluated the performance of the predictive methods over the entire time domain of a transient solution but also clearly revealed which SWCC predictive methods yielded conservative seepage analysis results. While general statements regarding the appropriateness of each SWCC predictive method cannot be made from the results of four comparisons alone, these results can aid in the selection of an SWCC predictive method.

5 How to Use Seep/W SWCC Prediction Add-in

This section describes where to place the SWCC prediction functions and in what format to input the various methods for successful use.

Installing Function (Add-In) in Seep/W

There are two directories that GeoStudio scans for Add-Ins. The first is located where the GeoStudio binaries are installed, usually the C drive; this is the location intended for core Add-Ins installation as part of the GeoStudio software product. The second location is where custom Add-Ins should be placed (Geo-Slope International 2012). The default location is in the "Application Data" directory, but it can be set to any directory specified. It is recommended that a directory be created in the "My Documents" folder as the new default location for GeoStudio Add-Ins. Specifying a new directory can be accomplished by navigating to Tools>Options in Geo-Studio and then browsing and selecting the location desired.

The file titled "SWCCprediction.dll" should be placed in the location set as the new default directory for Add-Ins in GeoStudio. Once this task has been completed, the five prediction methods are ready to be accessed. To perform a transient seepage analysis in Seep/W in the "KeyIn Analysis" screen, "Transient Analysis" must be selected and the settings, control, convergence, and time parameters adjusted as needed. Once the geometry and grid have been defined, the user should navigate to the "KeyIn Materials" screen, add a material, and select the "Saturated/Unsaturated Material Model." Once this is completed, the "Hydraulic Properties" parameters will appear. Selection of the KeyIn Volumetric Water Content button (labeled with three periods next to the volumetric water content pull-down menu) will bring up the "KeyIn Vol. Water Content Functions" screen. In the "Vol. Water Content Functions" screen, "Add a new function" should be selected and the function named accordingly. Once a new "Vol. Water Content Function" has been added, under the "Types" pull-down menu, "Add-In Function" should be chosen. In the Add-In field, "SWCC Prediction Functions" should be selected and the desired function chosen. Once the desired function has been chosen, the desired parameters must be entered, and "Close" selected. From the "Vol. Water

Content Fn" pull-down menu, the function that was given a unique name by the user should be selected. The following sections give guidance on the format of each of the prediction method's (function's) input parameters.

Note: Each of the five methods is programmed to use imperial units and will work as intended only if imperial units are used.

Method 1: (Zapata et al., 2000)

The SWCC prediction method outlined by Zapata et al. (2000) predicts the SWCC based on the following parameters:

- **porosity**: volume of voids divided by the total sample volume, input as a decimal
- **D60**: grain size for which 60% of the material is finer, required to be input in millimeters (mm)
- **PIpercent**: the plasticity index, input as a percent
- **percentPassing**: the percentage of material finer than the #200 sieve, expressed as a decimal

The default data correspond to a material with the following parameters: porosity is 0.5, D60 is 0.1 mm, PIpercent is 1.5, and percentPassing is 0.3. If the wPI value is greater than 0, then the D60 parameter is not needed.

The method as outlined in the main report makes a distinction between the fine-grained and the coarse-grained soils. A coarse-grained soil is defined as a soil with a wPI value equal to zero, where wPI is the product of the percent passing the #200 (expressed as a decimal) sieve and the plasticity index (expressed as a percent). This method predicts the drying curve of the SWCC, and this function's name is "Zapata_Imp."

Method 2: (Perera et al., 2005)

The SWCC prediction method outlined by Perera et al. (2005) predicts the SWCC based on the following parameters:

- **percentPassing**: the percentage of material finer than the #200 sieve, expressed as a decimal
- **D10, D20, D30, D60, D90**: the diameter (mm) of material at each percent passing. For example D10 is the grain size diameter for which 10% of the material is finer.

- **porosity**: the volume of voids divided by the total sample volume, input as a decimal.

Perera's method of SWCC prediction is an expansion of the work performed by Zapata et al. (2000). The coarse-grained soil parameters were expanded to better enhance the prediction of SWCC for these types of materials. A *coarse-grained soil* is defined as a soil whose wPI value is less than 1.0 and has the same parameter described in Zapata's method (Method 1). The function name is "Perera_Imp." The default material has the following parameters: porosity is 0.5, PIpercent is 15, and percentPassing is 0.3. If a material has a wPI value greater than 1.0, it is considered a fine-grained material; and the D10 through D90 values need not be assigned.

Method 3: (Sleep 2011)

Sleep's method of SWCC prediction is based on data extracted from the UNSODA database. Due to the use of the textural classification system used in the UNSODA database, the USCS classification is estimated by using the saturated hydraulic conductivity values. Unlike the other methods, this method allows the user to determine whether or not the function returns one of four curves: the wetting, the 90% confidence wetting, the drying, or the 90% confidence drying curves. The following parameters must be defined in order to predict the desired curve:

- **Curve**: a value of 1 to 4 corresponding to the desired curve:
    1. Average wetting curve
    2. 90% confidence wetting curve
    3. Average drying curve
    4. 90% confidence drying curve
- **ksat**: the saturated hydraulic conductivity value expressed in cm/s
- **porosity**: the volume of voids divided by the total sample, input as a decimal.

Clay materials with a hydraulic conductivity value less than 10^{-7} cm/s will be assigned the range of SWCCs used for the silt material. This is due to the absence of clay material in the UNSODA database. This function's name is "Sleep_Imp."

Method 4: (Tomasella and Hodnett 1998)

The Tomasella and Hodnett method predicts the SWCC based on the following parameters:

- **perClay:** the percent clay of the material, based on the textural classification (percent of particles finer than 0.002 mm,) expressed as a percent
- **perSilt:** the percent silt of the material, based on the textural classification (percent of particles finer than 0.05 mm but coarser than 0.002 mm)

The porosity is not an input parameter: the function predicts the porosity based on the two function input parameters, percent silt and clay. This function's name is "Tomasella_Imp"; this function predicts the drying SWCC.

Method 5: (Rawls et al. 1991)

Rawls's method of predicting the SWCC uses the following input parameters:

- **Porosity:** volume of voids divided by the total sample volume; it corresponds to the saturated volumetric water content, input as a decimal
- **perSand:** the percent sand of the material, based on the textural classification (percent particles finer the 2 mm but coarser than 0.05 mm), expressed as a percent
- **perClay:** the percent clay of the material, based on the textural classification (percent particles finer the 0.002 mm), expressed as a percent

This function's name is "Rawls_Imp"; this function predicts the drying SWCC.

6 Conclusion

Five soil water characteristic curve prediction methods were reviewed and compared to independent laboratory data over a range of soil types. The significance of the error in the predictive methods was assessed through transient seepage analyses. The relationship between matric suction and volumetric water content is of central importance when performing a transient seepage analysis. This relationship significantly impacts the soil hydraulic conductivity. The results of the numerical analysis show that, in general, the Rawls predictive method gives an adequate prediction of the SWCC over a range of material types. The results of the analyses also demonstrate that the closest SWCC prediction does not guarantee the best match to the transient analysis using the laboratory data curve: the shape of the curve and the AEV are also important.

The concept of a normalized saturation coefficient was developed to quantify the effects of parameter variation on transient seepage. The coefficient provides a convenient means of displaying the response of any geometry to a transient hydraulic loading. The saturation coefficient illustrated more of a difference between the measured SWCC results and the predicted SWCC results than was obtained by comparing pressure profiles at a fixed time. This is in part due to the short time duration for which pressure plots were generated. Nevertheless, the saturation coefficient curves show the propagation of the wetting front through the model in one continuous curve, reflecting the transient response of the whole geometry instead of just one location. From the results of these analyses, it became evident that only the method by Perrera et al. (2005) was conservative (or nearly so) for all four soil types. Further comparisons should be conducted on a larger data set of both natural and compacted soils to evaluate which methods are consistently conservative for various soil types.

A SEEP/W Add-In function that provides four methods of approximating the SWCC based on soil classification and index properties was developed. It is highly recommended that these predictive methods be used only for preliminary analysis, as they are not meant to replace laboratory-measured SWCC, but only to give an initial estimate. The results also indicate that when using a predictive method to derive the SWCC, it is imperative to know which predictive method works the best for the

particular soil that is to be analyzed. It seems that the best way to acquire this information is to investigate from which soil data set the predictive method was derived.

References

Askarinejad, A., F. Casini, P. Kienzler, and S. M. Springman. 2011. Comparison between the in situ and laboratory water retention curves for a silty sand. In *Unsaturated Soils-Proceedings of the 5th International Conference on Unsaturated Soils, 6-8 September, Barcelona, Spain,* 1:423-428.

ASTM. 2016. Standard practice for classification of soils for engineering purposes (Unified Soil Classification System). In *Annual Book of ASTM Standards*. ASTM 2487, 249-260. West Conshohocken, PA: American Society for Testing and Materials.

Aubertin, M., M. Mbonimpa, B. Bussiere, and R. P. Chapuis. 2003. A model to predict the water retention curve from basic geotechnical properties. *Canadian Geotechnical Journal* 40(6):1104-1122.

Cedergren, H. R. 1997. *Seepage, drainage, and flow nets*. Vol. 16. Hoboken, NJ: John Wiley & Sons.

Fredlund, D. G., H. Rahardjo, and M. D. Fredlund. 2012. *Unsaturated soil mechanics in engineering practice*. Hoboken, NJ: John Wiley & Sons.

Fredlund, D. G., and A. Xing. 1994. Equations for the soil-water characteristic curve. *Canadian Geotechnical Journal* 31(4):521-532.

Geo-Slope International Ltd. 2007. *SEEP/W. Version 7.23, user's guide*. Calgary, Alberta, Canada: GeoStudio.

Geo-Slope International Ltd. 2012. *Add-ins programming guide and reference*. Calgary, Alberta, Canada: GeoStudio.

Lam, L., and D. G. Fredlund. 1984. *Saturated-unsaturated transient finite element seepage model for geotechnical engineering*. Finite Elements in Water Resources. Berlin Heidelberg: Springer.

Leij, F. J. 1996. *The UNSODA unsaturated soil hydraulic database: user's manual*. Vol. 96, no. 95. National Risk Management Research Laboratory, Office of Research and Development. Washington, DC: U.S. Environmental Protection Agency.

Li, A. G., L. G. Tham, Z. Q. Yue, C. F. Lee, and K. T. Law. 2005. Comparison of field and laboratory soil-water characteristic curves. *Journal of Geotechnical and Geo-environmental Engineering* 131(9):1176-1180.

Likos, W. J., N. Lu, and J. W. Godt. 2013. Hysteresis and uncertainty in soil water-retention curve parameters. *Journal of Geotechnical and Geoenvironmental Engineering* 140(4), 04013050.

Lu, Ning, and W. J. Likos. 2004. *Unsaturated soil mechanics*. New York: John Wiley & Sons.

Nemes, A., M. G. Schaap, F. J. Leij, and J. H. M. Wösten. 2001. Description of the unsaturated soil hydraulic database UNSODA version 2.0. *Journal of Hydrology* 251(3):151-162.

Perera, Y. Y., C. E. Zapata, W. N. Houston, and S. L. Houston. 2005. *Prediction of the soil-water characteristic curve based on grain-size-distribution and index properties*. ASCE Geotechnical Special Publication 130. Reston, VA: American Society of Civil Engineers.

Rawls, W. J., D. L. Brakensiek, and K. E. Saxton. 1982. Estimation of soil water properties. *Transactions of the ASAE* 25(5):1316-1320.

Rawls, W. J., T. J. Gish, and D. L. Brakensiek. 1991. Estimating soil water retention from soil physical properties and characteristics. In *Advances in soil science*. New York: Springer.

Schaap, M. G., and F. J. Leij. 2000. Improved prediction of unsaturated hydraulic conductivity with the Mualem-van Genuchten model. *Soil Science Society of America Journal* 64(3):843-851.

Sleep, M. D. 2011. Analysis of transient seepage through levees. PhD diss., Virginia Polytechnic Institute and State University.

Song, Y. S., W. K. Hwang, S. J. Jung, and T. H. Kim. 2012. A comparative study of suction stress between sand and silt under unsaturated conditions. *Engineering Geology*, 124:90-97.

Tinjum, J. M., C. H. Benson, and L. R. Blotz. 1997. Soil-water characteristic curves for compacted clays. *Journal of Geotechnical and Geo-environmental Engineering* 123(11):1060-1069.

Terzaghi, Karl. 1996. *Soil mechanics in engineering practice*. New York: John Wiley & Sons.

Tomasella, J., and M. G. Hodnett. 1998. Estimating soil water retention characteristics from limited data in Brazilian Amazonia. *Soil Science* 163(3):190-202.

Tracy, F. T., T. L. Brandon, and M. K. Corcoran. 2016. *Transient seepage analyses in levee engineering practice*. ERDC TR-16-8. Vicksburg, MS: U.S. Army Engineer Research and Development Center.

van Genuchten, M. T. 1980. A closed-form equation for predicting the hydraulic conductivity of unsaturated soils. *Soil Science Society of America Journal* 44(5):892-898.

Zapata, C. E., W. N. Houston, S. L. Houston, and K. D. Walsh. 2000. *Soil-water characteristic curve variability*. ASCE Geotechnical Special Publication 99. Denver, CO: American Society of Civil Engineers.

REPORT DOCUMENTATION PAGE

Form Approved
OMB No. 0704-0188

1. REPORT DATE ***(DD-MM-YYYY)***
June 2017
(Revised November 2017)

2. REPORT TYPE
Final

3. DATES COVERED ***(From - To)***

4. TITLE AND SUBTITLE

SWCC Prediction: Seep/W Add-In Functions

5a. CONTRACT NUMBER

5b. GRANT NUMBER

5c. PROGRAM ELEMENT NUMBER

6. AUTHOR(S)

Lucas Walshire and Bryant Robbins

5d. PROJECT NUMBER
HFK2F2

5e. TASK NUMBER

5f. WORK UNIT NUMBER

7. PERFORMING ORGANIZATION NAME(S) AND ADDRESS(ES)

Geotechnical and Structures Laboratory
U.S. Army Engineer Research and Development Center
3909 Halls Ferry Road
Vicksburg, MS 39180-6199

8. PERFORMING ORGANIZATION REPORT NUMBER

ERDC/GSL SR-17-4 rev.

9. SPONSORING / MONITORING AGENCY NAME(S) AND ADDRESS(ES)

Headquarters, U.S. Army Corps of Engineers
Washington, DC 20314-1000

10. SPONSOR/MONITOR'S ACRONYM(S)
HQ-USACE

11. SPONSOR/MONITOR'S REPORT NUMBER(S)

12. DISTRIBUTION / AVAILABILITY STATEMENT
Approved for public release; distribution is unlimited.

13. SUPPLEMENTARY NOTES

14. ABSTRACT

The soil water characteristic curve (SWCC) defines a constitutive relationship between the negative pressure that develops when a soils saturation level is less than fully saturated, and the corresponding volume of water held in the pore space of the soil matrix. As this relationship is not commonly measured in geotechnical laboratories, practitioners often attempt to predict this relationship based on other commonly measured material properties using empirical prediction methods. The performance of five SWCC empirical predictors was evaluated through comparisons to independently measured SWCC data for four soils. SWCC prediction methods were selected for this investigation if they incorporated commonly measured soil properties to predict the SWCC. The error in the SWCC prediction was assessed in terms of both the mean squared error on the SWCC prediction and the impact of the error on a numerical analysis of the Green and Ampt infiltration problem. The results of the numerical analysis were assessed in terms of a normalized saturation coefficient. The normalized saturation coefficient provided a clear means of monitoring a transient seepage analysis through a single measure. Results indicate that the SWCC prediction methods yielding the lowest mean squared error did not necessarily yield the smallest error in the transient seepage analysis. Further, only the Perrera et al. method consistently yielded conservative analysis results for all soil types investigated.

15. SUBJECT TERMS

Soil physics
Soil moisture
Transient seepage
Soil water retention
Soil water characteristic curve
Soil infiltration rate
Soil matric potential
Seepage

16. SECURITY CLASSIFICATION OF:			**17. LIMITATION OF ABSTRACT**	**18. NUMBER OF PAGES**	**19a. NAME OF RESPONSIBLE PERSON**
a. REPORT	**b. ABSTRACT**	**c. THIS PAGE**			**19b. TELEPHONE NUMBER** ***(include area code)***
Unclassified	Unclassified	Unclassified		45	